Constraining Neutron Capture Cross Sections for Unstable Nuclei with Surrogate Reaction Data and Theory

J. E. Escher,[1,*] J. T. Harke,[1] R. O. Hughes,[1] N. D. Scielzo,[1] R. J. Casperson,[1] S. Ota,[2] H. I. Park,[2] A. Saastamoinen,[2] and T. J. Ross[3]

[1]*Nuclear and Chemical Sciences Division, Lawrence Livermore National Laboratory, Livermore, California 94551, USA*
[2]*Cyclotron Institute, Texas A&M University, College Station, Texas 77840, USA*
[3]*Department of Physics, University of Richmond, Richmond, Virginia 23173, USA*

(Received 18 September 2017; revised manuscript received 14 January 2018; published 31 July 2018)

Obtaining reliable data for nuclear reactions on unstable isotopes remains an extremely important task and a formidable challenge. Neutron capture cross sections—crucial ingredients for models of astrophysical processes, national security applications, and simulations of nuclear energy generation—are particularly elusive, as both projectile and target in the reaction are unstable. We demonstrate a new method for determining cross sections for neutron capture on unstable isotopes, using $^{87}\mathrm{Y}(n,\gamma)$ as a prototype. To validate the method, a benchmark experiment is carried out to obtain the known $^{90}\mathrm{Zr}(n,\gamma)$ cross section analogously. Our approach, which employs an indirect ("surrogate") measurement combined with theory, can be generalized to a larger class of nuclear reactions. It can be used both with traditional stable-beam experiments and in inverse kinematics at rare-isotope facilities.

DOI: 10.1103/PhysRevLett.121.052501

Neutron capture reactions play an important role in nuclear physics and other fields that seek to understand physical processes in which neutrons react with their environment. Knowledge of capture cross sections is a crucial component in our quest to understand the origin of the elements, one of the most compelling interdisciplinary challenges physicists seek to address [1–5]. The cross sections are required input for astrophysical models that describe stellar evolution and the synthesis of the elements heavier than iron and that aim at identifying the sites responsible for these nucleosynthesis processes. Capture cross sections are also essential for modeling processes relevant to generating energy [6] and for interpreting radiochemical data related to national security applications [7,8].

Many required capture cross sections are unknown and extremely difficult to determine experimentally, as their measurement involves colliding neutrons with short-lived or highly radioactive targets. The nuclear science community is addressing this challenge with significant investments in new experimental facilities. Around the world, powerful rare-isotope facilities are beginning to produce beams of very short-lived nuclei. These can be used in inverse-kinematics experiments to bombard longer-lived target materials. Neutrons are not suitable (stationary) target material [9]; thus, new techniques have to be developed to extract the desired cross sections from radioactive-beam experiments [10–16].

In this Letter, we present an approach for determining cross sections for capture reactions that proceed via an intermediate "compound" nucleus (CN). Calculations of compound cross sections are often quite limited in accuracy due to uncertainties in the nuclear physics inputs needed. The "surrogate reaction method" [10] is designed to provide experimental constraints for the models that describe the decay of the compound nucleus and that dominate the uncertainties of the calculations. The experimentally constrained calculations yield the desired capture cross sections, thus overcoming the challenges that direct measurements face. The approach can be used both with traditional stable-beam experiments (as presented here) and in inverse-kinematics experiments [17].

Our goal is to demonstrate the method for a short-lived isotope in a well-studied, but challenging, area of the isotopic chart and to provide an assessment of the approach by selecting a nearby isotope for a benchmark study. We focus on the neutron-capture reaction for the short-lived $^{87}\mathrm{Y}$ nucleus ($\tau_{1/2} = 79.8$ h) for which no direct measurements exist. We present data from a surrogate measurement that, when combined with theoretical modeling, yield the sought-after $^{87}\mathrm{Y}(n,\gamma)$ cross section. To provide a benchmark, we employ identical techniques to determine the known $^{90}\mathrm{Zr}(n,\gamma)$ cross section.

In the $^{87}\mathrm{Y}(n,\gamma)$ reaction, projectile (n) and target ($^{87}\mathrm{Y}$) fuse to form the highly excited compound nucleus ($^{88}\mathrm{Y}^{*}$), which subsequently decays by γ-ray emission [Figs. 1(a) and 1(b)]. The capture cross section can be written in the Hauser-Feshbach statistical reaction formalism [18]

$$\sigma_{n\gamma}(E_n) = \sum_{J,\pi} \sigma_n^{\mathrm{CN}}(E_{\mathrm{ex}}, J, \pi) G_\gamma^{\mathrm{CN}}(E_{\mathrm{ex}}, J, \pi), \qquad (1)$$

where $\sigma_n^{\mathrm{CN}} = \sigma_{\mathrm{CN}}(n + {}^{87}\mathrm{Y} \rightarrow {}^{88}\mathrm{Y}^*)$ denotes the cross section for forming the compound nucleus at excitation energy E_{ex} with angular-momentum J and parity π, and $G_\gamma^{\mathrm{CN}} = G^{\mathrm{CN}}({}^{88}\mathrm{Y}^* \rightarrow {}^{88}\mathrm{Y} + \gamma)$ is the probability for the decay of this state via the emission of one or more γ rays. The kinetic energy E_n of the neutron is related to the excitation energy of the compound nucleus E_{ex} via $E_n = (1 + 1/A)(E_{\mathrm{ex}} - S_n)$, where S_n is the energy required for separating a neutron from the nucleus ${}^{A+1}Z$ [see Fig. 1(b)]. The factored form in Eq. (1) embodies the essential assumptions of the Hauser-Feshbach model, that formation and decay of the compound nucleus are independent processes, and that the total spin and parity of the compound system must be conserved [19].

Here, as in many other reactions of interest, the formation cross section σ_n^{CN} can be calculated to a reasonable accuracy using neutron-nucleus effective interactions ("optical potentials"). The decay probabilities G_γ^{CN} are difficult to calculate accurately since they contain transmission coefficients and level densities for all competing decay channels. Transmission coefficients quantify the probability of a particle or γ ray escaping the CN, and level densities quantify the number of possible states that can be reached in this decay process [20,21]. The objective of the surrogate method is to constrain the decay probabilities G_γ^{CN} experimentally.

In the surrogate experiment, the CN is produced via an alternative reaction [Fig. 1(c)], here $p + {}^{89}\mathrm{Y} \rightarrow d + {}^{88}\mathrm{Y}^*$, and the outgoing deuteron (d) is detected. The deuteron angle θ_d and energy E_d determine the excitation energy E_{ex} at which ${}^{88}\mathrm{Y}^*$ was produced. A range of energies, including

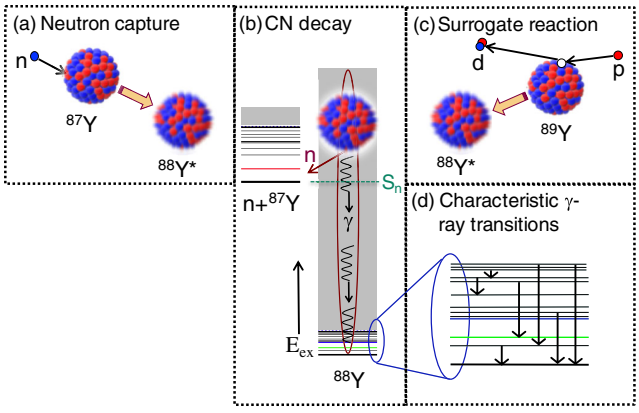

FIG. 1. Surrogate measurement of the ${}^{87}\mathrm{Y}(n,\gamma)$ cross section. Because of the short lifetime of ${}^{87}\mathrm{Y}$, the reaction cannot be measured directly. In the surrogate experiment, the first step of the capture reaction $n + {}^{87}\mathrm{Y} \rightarrow {}^{88}\mathrm{Y}^*$ (a) is replaced by the $p + {}^{89}\mathrm{Y} \rightarrow d + {}^{88}\mathrm{Y}^*$ reaction (c), which produces the same CN, ${}^{88}\mathrm{Y}^*$. The subsequent decay of ${}^{88}\mathrm{Y}^*$ (b) is then measured and used to extract the ${}^{87}\mathrm{Y}(n,\gamma)$ cross section. (d) γ rays associated with transitions between known levels of ${}^{88}\mathrm{Y}$ are used to identify the decay path.

$E_{\mathrm{ex}} > E_n$, must populated, so that the competition between γ emission, neutron emission, and other decay channels can be studied. In coincidence with the deuteron, the experiment measures observables that indicate how the CN ${}^{88}\mathrm{Y}^*$ has decayed. Here, characteristic γ transitions between low-lying levels in ${}^{88}\mathrm{Y}$ [see Fig. 1(d)] indicate capture, while transitions between levels in ${}^{87}\mathrm{Y}$ (not shown) indicate neutron emission. The measured coincidence probability can be expressed as

$$P_{\delta\gamma}(E_{\mathrm{ex}},\theta_d) = \sum_{J,\pi} F_\delta^{\mathrm{CN}}(E_{\mathrm{ex}},J,\pi,\theta_d) G_\gamma^{\mathrm{CN}}(E_{\mathrm{ex}},J,\pi), \quad (2)$$

where $F_\delta^{\mathrm{CN}}(E_{\mathrm{ex}},J,\pi,\theta_d)$ is the probability for forming ${}^{88}\mathrm{Y}^*$ in the surrogate reaction δ with specific values for E_{ex}, J, π. The distribution $F_\delta^{\mathrm{CN}}(E_{\mathrm{ex}},J,\pi,\theta_d)$ has to be determined theoretically, so that the $G_\gamma^{\mathrm{CN}}(E_{\mathrm{ex}},J,\pi)$ can be constrained. The latter is accomplished by modeling the decay of the CN and adjusting parameters in the model to reproduce the measured $P_{\delta\gamma}(E_{\mathrm{ex}},\theta_d)$ [10]. The desired cross section is then calculated using Eq. (1).

Past applications of the surrogate approach to neutron-induced fission assumed the decay probabilities $G_{\mathrm{fission}}^{\mathrm{CN}}(E_{\mathrm{ex}},J,\pi)$ to be independent of J, π [10,22,23]. This ("Weisskopf-Ewing") approximation, which removes the need to calculate $F_\delta^{\mathrm{CN}}(E_{\mathrm{ex}},J,\pi,\theta_d)$, has been shown to be a reasonable approximation for $(n,\ f)$ cross sections [24], but is known to break down for neutron-capture reactions [25–30], with the Zr-Y region showing particular sensitivity to spin-parity effects: sensitivity studies find that the Weisskopf-Ewing approximation leads to capture cross sections that deviate an order of magnitude from the known result and have the wrong shape. Here, we move beyond this approximation by fully accounting for the spin-parity dependence of the reaction.

The data were collected using the K150 Cyclotron at Texas A&M University. Natural ${}^{89}\mathrm{Y}$ and enriched ${}^{90,91,92,94,96}\mathrm{Zr}$ targets were bombarded by a 1.5-nA, 28.5-MeV proton beam. Backgrounds from carbon and oxygen in the targets were accounted for using a natural C target, which contained oxygen as a contaminant [27,31]. The energy and angular distributions of the outgoing deuterons were measured using the Silicon Telescope Array for Reaction Studies [32,33]. The coincident γ rays were detected with five HPGe clover detectors in the Livermore-Texas-Richmond array [27,32]. The detected deuteron energies were converted to nuclear excitation energy by accounting for energy losses in dead layers, the reaction Q value, and the nuclear recoil. The particle energy calibration was obtained using a ${}^{226}\mathrm{Ra}$ α source and confirmed by comparing against discrete lines appearing in the particle spectra from the target. The energy resolution was determined to be 80 keV (at 1σ uncertainty) from these features. $P_{\delta\gamma}$ was obtained by measuring N_δ, the total

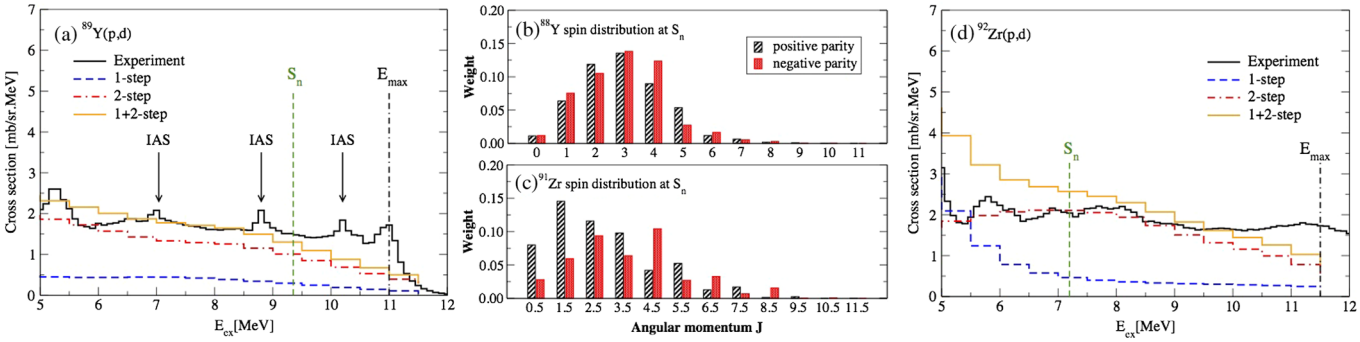

FIG. 2. Results of the (p, d) calculations. Cross section predictions, integrated over the angular range of the experiment ($\theta_d = 30°$–$60°$), are compared to data in (a) for $^{89}\mathrm{Y}(p,d)$ and (d) for $^{92}\mathrm{Zr}(p,d)$. One- and two-step contributions, and their sums, are shown. IAS are identified in the $^{89}\mathrm{Y}(p,d)$ case. The calculated spin-parity distributions $F_\delta^{\mathrm{CN}}(E_{\mathrm{ex}}, J, \pi)$ at the neutron separation energy are given in (b) for $^{88}\mathrm{Y}$ and in (c) for $^{91}\mathrm{Zr}$. The distributions change slowly between $E_{\mathrm{ex}} = 6$ and 11 MeV.

number of detected deuterons, and $N_{\delta\gamma}$, the number of coincidences between a deuteron and the γ ray that identifies the relevant exit channel: $P_{\delta\gamma}^{\mathrm{expt}}(E_{\mathrm{ex}}, \theta_d) = N_{\delta\gamma}(E_{\mathrm{ex}}, \theta_d)/N_\delta(E_{\mathrm{ex}}, \theta_d)\epsilon(E_\gamma)$. Here, $\epsilon(E_\gamma)$ denotes the photopeak efficiency for detecting the exit channel γ ray. Details on the detector arrays, data-acquisition system, and data analysis can be found in Refs. [31,34,35].

To calculate the surrogate spin-parity distribution $F_\delta^{\mathrm{CN}}(E_{\mathrm{ex}}, J, \pi, \theta_d)$ for the nucleus $^{88}\mathrm{Y}^*$, the one-neutron removal reaction $^{89}\mathrm{Y}(p,d)$ has to be described. This requires a reaction formulation as well as nuclear structure information.

The reaction is treated in the finite-range distorted-wave Born approximation (DWBA). In a first-order description, a neutron is picked up directly by the incoming proton and forms the deuteron that is detected. Well-known optical model potentials are used to describe the proton-^{89}Y and deuteron-^{88}Y interactions [36,37].

The structure of the orbital from which the neutron is removed enters the formalism. The orbitals relevant here are deeply bound and cannot be reliably described by current microscopic theories [38–43]. We therefore employ an approach [44] that uses (independent) elastic scattering data [45,46] to yield the requisite information.

The reaction description has to go beyond a first-order treatment: excitation energies up to $E_{\mathrm{ex}} \approx 10$–$12$ MeV make it necessary to include contributions from two-step reaction processes. The strongest contributions are from inelastic scattering in the entrance and exit channels: the incoming proton can excite the target prior to neutron removal; alternatively, the outgoing deuteron can excite the remnant ^{88}Y nucleus after neutron removal. We account for both processes: using the two-step DWBA mechanism implemented in the code FRESCO [47], we include $(p,p')(p',d)$ and $(p,d')(d',d)$ contributions. A vibrational collective model is employed to calculate the form factor for the inelastic scattering step. Inelastic excitations involving angular-momentum transfers up to $8\hbar$ were considered and their strength was adjusted to reproduce known inelastic scattering cross sections. The angular momenta of the target, inelastic excitations, and hole states are coupled to yield final spins J_f, where J_f reaches values up to 11 for two-step processes [see Figs. 2(b) and 2(c)], while the one-step mechanism can only reach up to $J_f = 5$. At the high E_{ex} relevant here, the reaction populates a large number of final states in any given energy interval, so the contributions add incoherently. Our assumptions are similar to those underlying successful quantum-mechanical pre-equilibrium theories [48–50].

The sum of all calculated one- and two-step contributions is compared to the measured (p, d) cross section in Fig. 2(a) for $^{89}\mathrm{Y}(p,d)$ and Fig. 2(d) for $^{92}\mathrm{Zr}(p,d)$. The present model aims at describing the energy regime around 6–12 MeV. Here, two-step contributions are seen to dominate the cross section. The calculations reproduce the measured cross sections in the energy range $E_{\mathrm{ex}} = 6 - 10$ MeV well and underpredict the data at $E_{\mathrm{ex}} = 10 - 12$ MeV.

The $^{89}\mathrm{Y}(p,d)$ reaction populates isobaric analog states (IAS), as indicated in Fig. 2(a). These are special excited states in ^{88}Y [51]. Their structure is closely connected to the structure of low-lying states in the neighboring ^{88}Sr nucleus; hence, we know their spins and parities. The present reaction description does not include transfers to IAS, but we account for their impact on the spin-parity distributions by determining from the data the enhancements above the smooth portion of the cross section and similarly enhancing the relevant spin-parity component. No evidence for IAS in ^{91}Zr is seen in the data; they are expected to occur at energies higher than relevant here.

We assume that the spin-parity distribution produced in the initial $1+2$-step reaction is representative of the distribution of the equilibrated nucleus prior to decay. The weights $F_\delta^{\mathrm{CN}}(E_{\mathrm{ex}}, J, \pi)$ shown in Figs. 2(b) and 2(c) are obtained by calculating the contribution of each final angular momentum to the total (p, d) cross section. The IAS

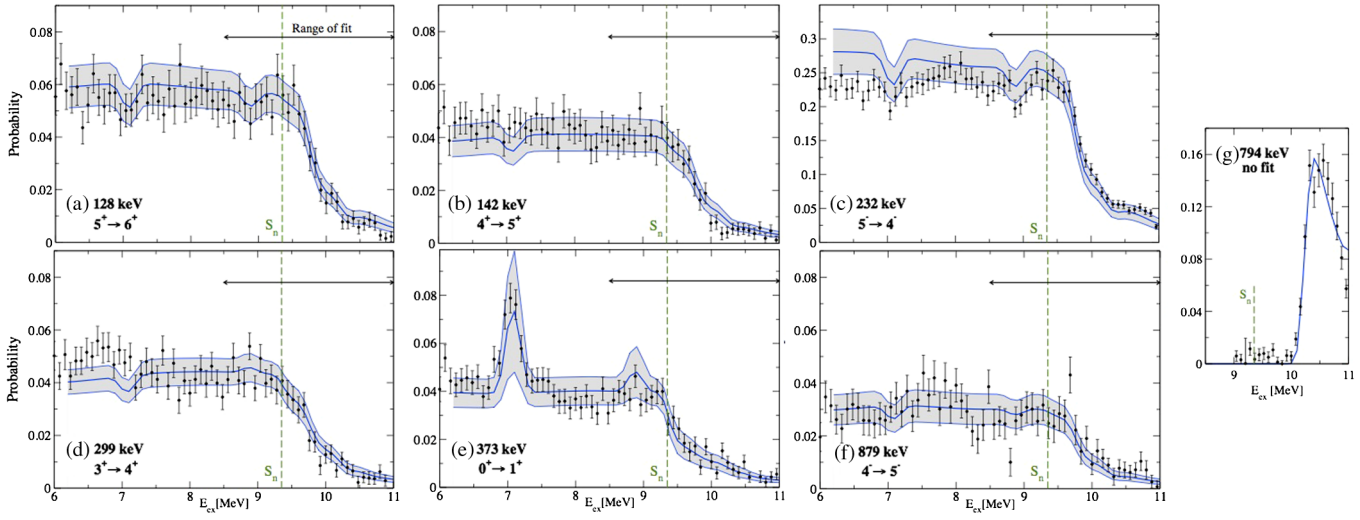

FIG. 3. Probabilities for observing specific γ-ray transitions in coincidence with the outgoing deuteron. Results of the fit (gray 1σ bands) are compared to experimental data (black symbols). Fitting range and separation energy S_n are indicated. (a)–(f) Transitions in ^{88}Y; (g) gives a transition in ^{87}Y. IAS contributions result in dips or peaks at specific energies.

contributions are added to this and the resulting distribution is used in a Hauser-Feshbach-type calculation that models the CN decay.

With $F_\delta^{\mathrm{CN}}(E_{\mathrm{ex}}, J, \pi)$ obtained in this manner, we can derive constraints for the decay models, using the measured coincidence probabilities $P_{\delta\gamma}^{\mathrm{expt}}$ and Eq. (2). We express the $G_\gamma^{\mathrm{CN}}(E_{\mathrm{ex}}, J, \pi)$ in terms of well-established functional forms for level densities and transmission coefficients [20,52], with parameters that are to be determined. Sensitivity studies establish reasonable parameter ranges: the level density model [53] used has four (five) adjustable parameters for ^{88}Y (^{91}Zr). The γ-ray transmission coefficient is dominated by electric and magnetic dipole transitions, requiring nine parameters to be varied [52,54–56]. The neutron transmission coefficients are known quite accurately for the nuclei considered [36] and are not varied. For isotopes far from stability, where transmission coefficients are less well known, such variations should be carried out. To account for uncertainties in the calculated $F_\delta^{\mathrm{CN}}(E_{\mathrm{ex}}, J, \pi)$, we vary the weights schematically by shifting the overall distribution by $\pm 1\hbar$.

Each parameter set leads to *predicted* coincidence probabilities according to Eq. (2). A comparison with the *measured* probabilities then leads to the sought-after parameter constraints. In practice, this comparison is carried out using a Bayesian Monte Carlo approach [57,58], which allows us to simultaneously account for uncertainties in the data, the structure information utilized, and shortcomings in the theoretical description. The procedure yields the desired (n, γ) cross section, along with its uncertainty.

Six γ-ray transitions in ^{88}Y are used to determine the ^{88}Y* decay parameters. To emphasize the energy region of interest to neutron capture, data from 0.5 MeV below to 1.5 MeV above the neutron separation energy are utilized. Data at lower energies serve as a check for the quality of the approach. Figures 3(a)–3(f) show that all transitions are simultaneously well reproduced, even at the lower energies. The effects of the IAS are clearly seen and reproduced. As an additional check, we compare a predicted and measured γ-ray transition in ^{87}Y [see Fig. 3(g)]. The extracted $^{87}\mathrm{Y}(n,\gamma)$ cross section, shown in Fig. 4, is higher than existing evaluations, which rely on regional systematics, and has a 1σ uncertainty of about $\pm 25\%$.

For the $^{90}\mathrm{Zr}(n,\gamma)$ case, we use five γ transitions and, again, restrict our fit to data around the separation energy ($S_n = 7.19$ MeV). The fit reproduces the data well in the energy range of interest (Fig. 5). The resulting $^{90}\mathrm{Zr}(n,\gamma)$ cross section, shown in (f), agrees with available direct measurements and evaluations, both in shape and magnitude. Its average is about a factor 2 larger than the data, but

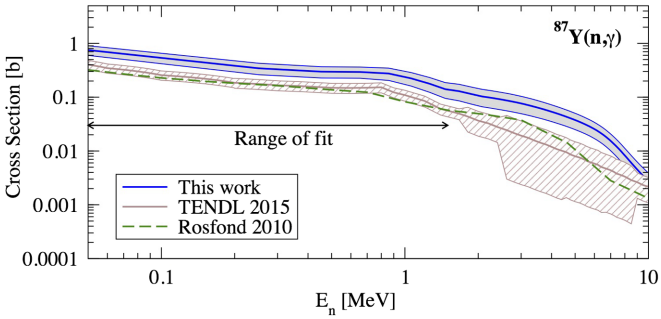

FIG. 4. The $^{87}\mathrm{Y}(n,\gamma)$ cross section, extracted from the surrogate data, with 1σ uncertainty (blue curves, gray band). The TENDL 2015 (brown curves, with hatched 1σ uncertainty) and Rosfond 2010 evaluations are based on regional systematics [59–61]. No direct measurements exist.

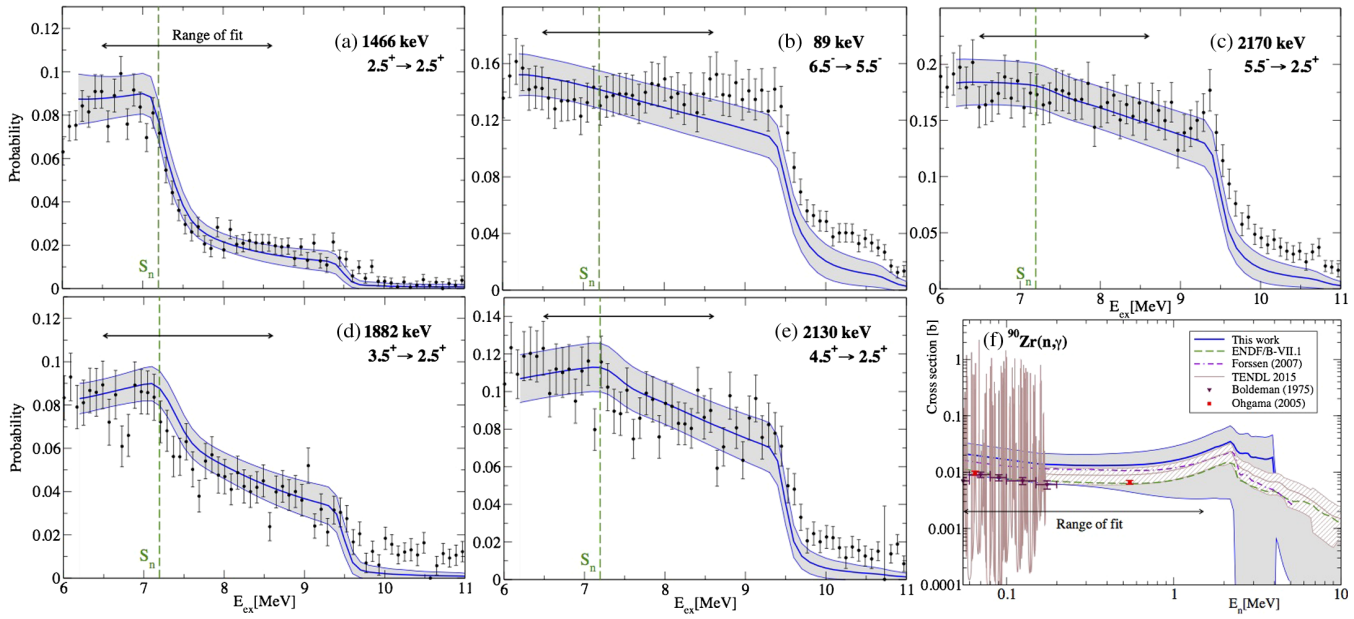

FIG. 5. Results for Zr. (a)–(e) Coincidence probabilities used in the fit. (f) The extracted $^{90}\mathrm{Zr}(n,\gamma)$ cross section is compared to direct measurements and several evaluations [25,62–65]. The Forssen calculation used D_0 and $\langle\Gamma_\gamma\rangle$ data, which are typically used—along with cross section data–to constrain (n,γ) calculations. TENDL (shown with hatched uncertainty band) and ENDF introduced further adjustments to agree more closely with the direct data.

encompasses the latter within its 1σ uncertainty. The result is a significant improvement over previous attempts to determine capture cross sections from surrogate reaction data and is notable since it is achieved for an isotope that is very sensitive to spin-parity effects [26].

To summarize, we have presented a new approach for determining neutron-capture cross sections for unstable isotopes using a combination of surrogate reaction data and theory. We have demonstrated that a theoretical description of the surrogate reaction is key to overcoming the limitations encountered in previous applications of this approach. The method makes no use of auxiliary constraining quantities, such as neutron resonance data, or average radiative widths, which are not available for short-lived isotopes. This approach will open up the possibility of determining unknown cross sections, with far-reaching implications for improving our understanding of stellar evolution and nucleosynthesis of the heavy elements: near stability, stable-beam experiments can be used to determine cross sections that shed light on the slow neutron-capture process (s process) [66], while further away from stability, radioactive beam experiments can provide reaction data relevant to rapid-neutron-capture (r process) nucleosynthesis [67].

Our approach of predicting F_δ^{CN} and determining the unknown decay parameters from Eq. (2) can be adapted to determine other cross sections of interest. For example, proton and α capture can be treated in direct analogy to the cases presented here. Furthermore, other surrogate reaction mechanisms can be used to form the CN, including inelastic scattering and reactions that transfer nucleons *to* the target: for the $(d,\ p)$ reaction, a prime candidate for inverse-kinematic experiments, a reaction description has recently been developed [68–70] and surrogate benchmark tests are underway [17,71]. Thus, the present work establishes a more general procedure for obtaining cross sections for short-lived nuclei from light-ion surrogate reactions.

We recognize the multiple contributions our friend and collaborator Cornelius Beausang made to this effort. We thank M. Dupuis, T. Bailey, B. Beck, A. C. Dreyfuss, R. Soltz, I. J. Thompson, C. Tong, and M. A. E. Williams for valuable discussions and A. Koning for the TENDL comparison data. This work was performed under the auspices of the U.S. Department of Energy by Lawrence Livermore National Laboratory under Contract DE-AC52-07NA27344.

*Corresponding author.
escher1@llnl.gov

[1] National Research Council, *Nuclear Physics: Exploring the Heart of Matter* (The National Academies Press, Washington, DC, 2013).

[2] Nuclear Science Advisory Committee, Reaching for the Horizon: The 2015 Long Range Plan for Nuclear Science (2015), https://science.energy.gov/~/media/np/nsac/pdf/2015LRP/2015_LRPNS_091815.pdf.

[3] A. Arcones, D. W. Bardayan, T. C. Beers, L. A. Bernstein, J. C. Blackmon, B. Messer, B. A. Brown, E. F. Brown, C. R. Brune, A. E. Champagne *et al.*, Prog. Part. Nucl. Phys. **94**, 1 (2017).

[4] M. Mumpower, R. Surman, G. McLaughlin, and A. Aprahamian, Prog. Part. Nucl. Phys. **86**, 86 (2016).
[5] H. Schatz, J. Phys. G **43**, 064001 (2016).
[6] N. Colonna, F. Belloni, E. Berthoumieux, M. Calviani, C. Domingo-Pardo, C. Guerrero, D. Karadimos, C. Lederer, C. Massimi, C. Paradela *et al.*, Energy Environ. Sci. **3**, 1910 (2010).
[7] F. N. Mortensen, J. M. Scott, and S. A. Colgate, Los Alamos Sci. **28**, 38 (2003).
[8] M. May, R. Abedin-Zadeh, D. Barr, A. Carnesale, P. E. Coyle, J. Davis, W. Dorland, W. Dunlop, S. Fetter, A. Glaser *et al.*, Nuclear Forensics Working Group of the American Physical Society's Panel on Public Affairs and the American Association for the Advancement of Science, Technical Report (2008), https://www.aps.org/policy/reports/popa-reports/upload/nuclear-forensics.pdf.
[9] R. Reifarth and Y. A. Litvinov, Phys. Rev. ST Accel. Beams **17**, 014701 (2014).
[10] J. E. Escher, J. T. Harke, F. S. Dietrich, N. D. Scielzo, I. J. Thompson, and W. Younes, Rev. Mod. Phys. **84**, 353 (2012).
[11] J. E. Escher, A. P. Tonchev, J. T. Burke, P. Bedrossian, R. J. Casperson, N. Cooper, R. O. Hughes, P. Humby, R. S. Ilieva, S. Ota *et al.*, Eur. Phys. J. Web Conf. **122**, 12001 (2016).
[12] H. Utsunomiya, S. Goriely, H. Akimune, H. Harada, F. Kitatani, S. Goko, H. Toyokawa, K. Yamada, T. Kondo, O. Itoh *et al.*, Phys. Rev. C **81**, 035801 (2010).
[13] R. Raut, A. P. Tonchev, G. Rusev, W. Tornow, C. Iliadis, M. Lugaro, J. Buntain, S. Goriely, J. H. Kelley, R. Schwengner *et al.*, Phys. Rev. Lett. **111**, 112501 (2013).
[14] A. Spyrou, S. N. Liddick, A. C. Larsen, M. Guttormsen, K. Cooper, A. C. Dombos, D. J. Morrissey, F. Naqvi, G. Perdikakis, S. J. Quinn *et al.*, Phys. Rev. Lett. **113**, 232502 (2014).
[15] S. N. Liddick, A. Spyrou, B. P. Crider, F. Naqvi, A. C. Larsen, M. Guttormsen, M. Mumpower, R. Surman, G. Perdikakis, D. L. Bleuel *et al.*, Phys. Rev. Lett. **116**, 242502 (2016).
[16] C. Guerrero, C. Domingo-Pardo, F. Käppeler, J. Lerendegui-Marco, F. R. Palomo, J. M. Quesada, and R. Reifarth, Eur. Phys. J. A **53**, 87 (2017).
[17] A. Ratkiewicz, J. Cizewski, S. Pain, A. Adekola, J. Burke, R. Casperson, N. Fotiades, M. McCleskey, S. Burcher, C. Shand *et al.*, Eur. Phys. J. Web Conf. **93**, 02012 (2015).
[18] W. Hauser and H. Feshbach, Phys. Rev. **87**, 366 (1952).
[19] Deviations from the factorized form can be accounted for by including width fluctuation corrections. To simplify the notation, they are omitted here, but are included in the calculations.
[20] P. Fröbrich and R. Lipperheide, *Theory of Nuclear Reactions* (Clarendon Press, Oxford, 1996).
[21] H. Hoffmann, *The Physics of Warm Nuclei* (Oxford University Press, New York, 2008).
[22] G. Kessedjian, B. Jurado, M. Aiche, G. Barreau, A. Bidaud, S. Czajkowski, D. Dassié, B. Haas, L. Mathieu, L. Audouin *et al.*, Phys. Lett. B **692**, 297 (2010).
[23] J. J. Ressler, J. T. Harke, J. E. Escher, C. T. Angell, M. S. Basunia, C. W. Beausang, L. A. Bernstein, D. L. Bleuel, R. J. Casperson, B. L. Goldblum *et al.*, Phys. Rev. C **83**, 054610 (2011).
[24] J. E. Escher and F. S. Dietrich, Phys. Rev. C **74**, 054601 (2006).
[25] C. Forssén, F. S. Dietrich, J. Escher, R. D. Hoffman, and K. Kelley, Phys. Rev. C **75**, 055807 (2007).
[26] J. E. Escher and F. S. Dietrich, Phys. Rev. C **81**, 024612 (2010).
[27] N. D. Scielzo, J. E. Escher, J. M. Allmond, M. S. Basunia, C. W. Beausang, L. A. Bernstein, D. L. Bleuel, J. T. Harke, R. M. Clark, F. S. Dietrich *et al.*, Phys. Rev. C **81**, 034608 (2010).
[28] S. Chiba and O. Iwamoto, Phys. Rev. C **81**, 044604 (2010).
[29] G. Boutoux, B. Jurado, V. Méot, O. Roig, L. Mathieu, M. Aïche, G. Barreau, N. Capellan, I. Companis, S. Czajkowski *et al.*, Phys. Lett. B **712**, 319 (2012).
[30] Q. Ducasse, B. Jurado, M. Aïche, P. Marini, L. Mathieu, A. Görgen, M. Guttormsen, A. C. Larsen, T. Tornyi, J. N. Wilson *et al.*, Phys. Rev. C **94**, 024614 (2016).
[31] S. Ota, J. T. Harke, R. J. Casperson, J. E. Escher, R. O. Hughes, J. J. Ressler, N. D. Scielzo, I. J. Thompson, R. A. E. Austin, B. Abromeit *et al.*, Phys. Rev. C **92**, 054603 (2015).
[32] S. R. Lesher, L. Phair, L. A. Bernstein, D. L. Bleuel, J. T. Burke, J. A. Church, P. Fallon, J. Gibelin, N. D. Scielzo, and M. Wiedeking, Nucl. Instrum. Methods Phys. Res., Sect. A **621**, 286 (2010).
[33] http://www.micronsemiconductor.co.uk.
[34] R. J. Casperson, J. T. Harke, N. D. Scielzo, J. E. Escher, E. McCleskey, M. McCleskey, A. Saastamoinen, A. Spiridon, A. Ratkiewicz, A. Blanc *et al.*, Phys. Rev. C **90**, 034601 (2014).
[35] R. O. Hughes, J. T. Harke, R. J. Casperson, J. E. Escher, S. Ota, J. J. Ressler, N. D. Scielzo, R. A. E. Austin, B. Abromeit, N. J. Foley *et al.*, Phys. Rev. C **93**, 024315 (2016).
[36] A. J. Koning and J.-P. Delaroche, Nucl. Phys. **A713**, 231 (2003).
[37] W. W. Daehnick, J. D. Childs, and Z. Vrcelj, Phys. Rev. C **21**, 2253 (1980).
[38] S. Galés, E. Hourani, S. Fortier, H. Laurent, J. M. Maison, and J. P. Schapira, Nucl. Phys. **A288**, 221 (1977).
[39] K. Hisamochi, O. Iwamoto, A. Kisanuki, S. Budihardjo, S. Widodo, A. Nohtomi, Y. Uozumi, T. Sakae, M. Matoba, M. Nakano *et al.*, Nucl. Phys. **A564**, 227 (1993).
[40] G. Duhamel, G. Perrin, J. P. Didelez, E. Gerlic, H. Langevin-Joliot, J. Guillot, and J. V. de Wiele, J. Phys. G **7**, 1415 (1981).
[41] G. Duhamel-Chrétien, G. Perrin, C. Perrin, V. Comparat, E. Gerlic, S. Gales, and C. P. Massolo, Phys. Rev. C **43**, 1116 (1991).
[42] P.-O. Söderman, J. Blomgren, A. Ringbom, N. Olsson, L. Nilsson, J. Bordewijk, S. Brandenburg, G. van't Hof, M. Hofstee, H. van der Ploeg *et al.*, Nucl. Phys. **A587**, 55 (1995).
[43] N. D. Thao, V. G. Soloviev, C. Stoyanov, and A. I. Vdovin, J. Phys. G **10**, 517 (1984).
[44] C. Mahaux and R. Sartor, *Advances in Nuclear Physics* (Springer, New York, 1991), Vol. 20, p. 1.
[45] J. P. Delaroche, Y. Wang, and J. Rapaport, Phys. Rev. C **39**, 391 (1989).
[46] O. V. Bespalova, I. N. Boboshin, V. V. Varlamov, T. A. Ermakova, B. S. Ishkhanov, E. A. Romanovsky, T. I. Spasskaya, and T. P. Timokhina, Phys. At. Nucl. **69**, 796 (2006).
[47] I. J. Thompson, Comput. Phys. Rep. **7**, 167 (1988).

[48] T. Tamura, T. Udagawa, and H. Lenske, Phys. Rev. C **26**, 379 (1982).
[49] A. Gattone, A. Ferrero, and O. Dragun, Nucl. Phys. **A424**, 1 (1984).
[50] E. Gadioli and P. E. Hodgson, *Pre-Equilibrium Nuclear Reactions* (Clarendon Press, Oxford, 1992).
[51] N. Auerbach, J. Hüfner, A. K. Kerman, and C. M. Shakin, Rev. Mod. Phys. **44**, 48 (1972).
[52] R. Capote, M. Herman, P. Oblozinský, P. Young, S. Goriely, T. Belgya, A. Ignatyuk, A. Koning, S. Hilaire, V. Plujko *et al.*, Nucl. Data Sheets **110**, 3107 (2009).
[53] A. Gilbert and A. G. W. Cameron, Can. J. Phys. **43**, 1446 (1965).
[54] R. Schwengner, G. Rusev, N. Tsoneva, N. Benouaret, R. Beyer, M. Erhard, E. Grosse, A. R. Junghans, J. Klug, K. Kosev *et al.*, Phys. Rev. C **78**, 064314 (2008).
[55] H. Utsunomiya, S. Goriely, T. Kondo, T. Kaihori, A. Makinaga, S. Goko, H. Akimune, T. Yamagata, H. Toyokawa, T. Matsumoto *et al.*, Phys. Rev. Lett. **100**, 162502 (2008).
[56] M. R. Mumpower, T. Kawano, J. L. Ullmann, M. Krtička, and T. M. Sprouse, Phys. Rev. C **96**, 024612 (2017).
[57] A. J. Koning, Eur. Phys. J. A **51**, 184 (2015).
[58] C. Tong, *PSUADE User's Manual. LLNL-SM-407882* (Lawrence Livermore National Laboratory, Livermore, CA, 2005).
[59] M. Nikolaev, http://www.nndc.bnl.gov/exfor/.
[60] A. Koning, Nucl. Data Sheets **123**, 207 (2015).
[61] A. Koning, D. Rochman, J. Kopecky, J. C. Sublet, E. Bauge, S. Hilaire, P. Romain, B. Morillon, H. Duarte, S. van der Marck *et al.*, Tendl-2015: Talys-Based Evaluated Nuclear Data Library, https://tendl.web.psi.ch/tendl_2015/tendl2015.html (2015).
[62] A. Koning (private communication).
[63] M. Chadwick, M. Herman, P. Obložinský, M. Dunn, Y. Danon, A. Kahler, D. Smith, B. Pritychenko, G. Arbanas, R. Arcilla *et al.*, Nucl. Data Sheets **112**, 2887 (2011).
[64] J. Boldeman, B. Allen, A. de L. Musgrove, and R. Macklin, Nucl. Phys. **A246**, 1 (1975).
[65] K. Ohgama, M. Igashira, and T. Ohsaki, AIP Conf. Proc. **819**, 373 (2006).
[66] F. Käppeler, R. Gallino, S. Bisterzo, and W. Aoki, Rev. Mod. Phys. **83**, 157 (2011).
[67] E. M. Burbidge, G. R. Burbidge, W. A. Fowler, and F. Hoyle, Rev. Mod. Phys. **29**, 547 (1957).
[68] G. Potel, F. M. Nunes, and I. J. Thompson, Phys. Rev. C **92**, 034611 (2015).
[69] J. Lei and A. M. Moro, Phys. Rev. C **92**, 044616 (2015).
[70] B. V. Carlson, R. Capote, and M. Sin, Few-Body Syst. **57**, 307 (2016).
[71] G. Potel, G. Perdikakis, B. V. Carlson, M. C. Atkinson, W. Dickhoff, J. E. Escher, M. S. Hussein, J. Lei, W. Li, A. O. Macchiavelli *et al.*, Eur. Phys. J. A **53**, 178 (2017).